Model-Based Control for Deploying a Servicing Deputy via a Space Manipulator

Sarah Hudson* and Donghoon Kim†
Department of Aerospace Engineering & Engineering Mechanics
University of Cincinnati
Cincinnati, OH, USA
Email: *hudsons5@mail.uc.edu, †donghoon.kim@uc.edu

Distribution Statement A. Approved for public release: distribution is unlimited (AFRL-2026-3313).

***Abstract*—Servicing space satellites presents significant challenges, particularly with increasing debris and satellite obsolescence. A promising solution involves utilizing a high-degree-of-freedom space manipulator system to deploy a deputy satellite for maintenance, inspection, and debris removal. This work proposes an approach that leverages the manipulator's throwing motion to launch the deputy toward a client satellite, reducing fuel consumption and improving accessibility for orbital maintenance. In simulations, the deputy is released from a chief satellite in geostationary orbit toward a client satellite, targeting a 3-hour rendezvous over a distance of 1 km. The mission achieves this with imparted velocities of approximately 10 cm/s, assuming no external thrusters are used for deputy attitude or trajectory control.**

***Index Terms*—CubeSats, Manipulators, Servicing, Deployment, Rendezvous**

I. Introduction

As more satellites are deployed into space, the increasing density of orbiting bodies raises the risk of collisions. Particularly in low Earth orbit, the growing number of satellites significantly increases the amount of space debris, which in turn exacerbates the need for effective spacecraft maintenance to prevent systems from becoming obsolete. This phenomenon, known as Kessler syndrome [1], describes the critical threshold at which cascading debris collisions pose a serious threat to new satellite deployments and the long-term sustainability of space operations.

Traditionally, astronauts have been sent into space to perform maintenance tasks on systems such as the International Space Station. While astronauts play an essential role in space missions, extravehicular activities expose them to hazardous conditions, including radiation [2], micro-meteoroid impacts [3], and extreme temperature fluctuations [4]. To mitigate these risks, recent research has explored the use of autonomous spacecraft for maintenance and inspection tasks [5]. In particular, CubeSats offer a cost-effective solution [6]. However, their compact design imposes significant limitations on onboard propulsion and power availability [7], which restricts their maneuverability for servicing missions.

This material is based on research sponsored by Air Force Research Laboratory (AFRL) under agreement number FA9453-24-2-0004. The U.S. Government is authorized to reproduce and distribute reprints for Governmental purposes notwithstanding any copyright notation thereon. The views and conclusions contained herein are those of the authors and should not be interpreted as necessarily representing the official policies or endorsements, either expressed or implied, of Air Force Research Laboratory (AFRL) and or the U.S. Government.

Recent efforts have proposed modular spacecraft architectures to support on-orbit servicing throughout a satellite's life cycle [8]. Rather than designing for fixed lifespans, these architectures emphasize adaptability, allowing components to be swapped during servicing or interchanged to accommodate evolving mission requirements. This approach replaces traditional monolithic designs with standardized modules, improving maintainability and extending operational life. The concept of using robotic manipulators in space is not novel. In 2007, the Defense Advanced Research Projects Agency collaborated with the National Aeronautics and Space Administration to develop the Orbital Express system [9]. The servicing vehicle in this system employed a robotic manipulator to perform maintenance tasks. While this approach provides maximum flexibility due to the high Degree-Of-Freedom (DOF) arm, it can reduce efficiency because it requires more complex planning. In the case of Orbital Express, the 6-DOF manipulator was used to autonomously transfer battery units and capture an unconstrained client [10]. The benefits of manipulators in space robotics include increased autonomy, expanded operational capability, and flexibility under off-nominal mission conditions. When combined with CubeSats performing inspection tasks [11], this forms an efficient strategy for extending the operational life of deployed satellites.

This work proposes an approach for autonomous satellite servicing using small CubeSat deputies. Instead of relying solely on onboard propulsion, a robotic manipulator mounted on a host satellite imparts a controlled throwing motion to the CubeSat, providing the necessary change in velocity ($\Delta\mathbf{v}$) to reach its desired location. This approach reduces the CubeSats' dependence on onboard thrusters, conserving valuable space within their constrained volume. By minimizing the need for onboard fuel, this method enhances the feasibility of CubeSats for autonomous maintenance and inspection in space.

II. Problem Definition

With the motivation for autonomous satellite servicing established, the key components of the system are defined. The

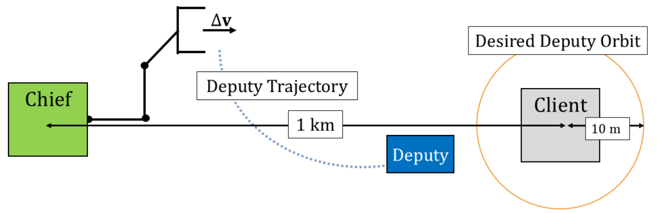

Fig. 1. Diagram showing the interaction between the Deputy and the Chief's manipulator, and the intended goal relative to the Client.

"Client" is the satellite requiring servicing. The "Chief" is the host satellite, equipped with a robotic manipulator that carries "Deputies," typically CubeSats, which are deployed to perform servicing operations (see Fig. 1). The "Desired Deputy Orbit" is the intended destination of the Deputy relative to the Client. This study evaluates the feasibility of using a manipulator to impart $\Delta\mathbf{v}$ to the Deputy for autonomous on-orbit servicing.

The problem is divided into several steps to simplify the interaction between the Chief and the Deputy:

1) The Deputy is held within the gripper.
2) The Deputy is released with a calculated $\Delta\mathbf{v}$.
3) The Deputy flies passively toward the Desired Deputy Orbit for servicing operations.

The following key assumptions are made:

- **Chief**: The base satellite is unactuated and free-floating.
- **Deputy**: It is a fully passive satellite and is initially rigidly attached to the gripper.
- **Servicer Orbit**: The Chief and Client occupy the same circular geostationary orbit.
- **Initial State**: The Chief and Client are positioned 1 km apart in the same orbit.
- **Deployment**: The manipulator imparts the required $\Delta\mathbf{v}$ with ideal separation.
- **Dynamics**: The system is simplified to planar motion.

III. Methodology

Given the complexity of launching a deputy via a robotic manipulator for a servicing mission, careful planning is required at each stage. From defining the problem to formulating the mathematical model and developing a preliminary simulation to predict system behavior, each step enhances understanding of mission feasibility.

Accurate modeling and control of the system require the definition of several reference frames: the inertial frame N, the base frame B, the End-Effector (EE) frame E, the Deputy frame D, and the i-th joint frame J_i. Each frame origin is denoted by O with the corresponding subscript (e.g., O_N for the inertial origin). The inertial frame is centered at the base satellite's center of mass at the initial condition. For simplicity, the origin notation O is omitted in vector definitions. Frame transformations are expressed using direction cosine matrices (e.g., C_{ED} maps vectors from D to E).

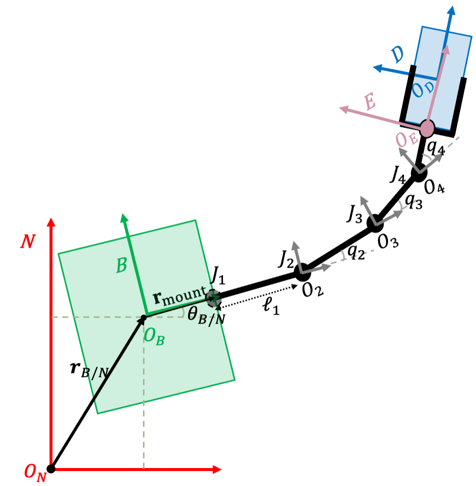

Fig. 2. Description of body frames and their relationships.

A. Kinematics & Dynamics

This work considers a free-floating base satellite equipped with a four-link planar manipulator. The first link is rigidly attached to the base and is unactuated, while links 2–4 are actuated. The system state vector $\mathbf{q} \in \mathbb{R}^6$ is defined as:

$$\mathbf{q} = \begin{bmatrix} {}^{N}\mathbf{r}_{B/N} \\ {}^{B}\theta_{B/N} \\ {}^{J}\mathbf{q}_m \end{bmatrix} \tag{1}$$

where $\mathbf{r}_{B/N} \in \mathbb{R}^2$ is the base's position relative to N, $\theta_{B/N}$ denotes the base's orientation relative to N, and $\mathbf{q}_m = [q_2\ q_3\ q_4]^T \in \mathbb{R}^3$ represents the manipulator's joint angles relative to the previous joint frame. The superscript denotes the expression in the corresponding frame. For simplicity, the superscript N is omitted.

To control the EE's position and velocity, the kinematics are formulated in N. Fig. 2 illustrates the reference frames and their relationships. The system is modeled sequentially from B through J_i to E. The joint and EE frames are represented as J_i and E.

B. Frame Definition

The forward kinematics, obtained by differentiating the EE position $\mathbf{r}_{E/N}$, yield the EE velocity:

$$\mathbf{v}_{E/N} = \mathcal{J}\dot{\mathbf{q}} \tag{2}$$

and the corresponding inverse kinematics are given by:

$$\dot{\mathbf{q}} = \mathcal{J}^{\dagger}\mathbf{v}_{E/N} \tag{3}$$

where $\mathcal{J} \in \mathbb{R}^{6\times 6}$ is the geometric Jacobian, and $\mathcal{J}^{\dagger}$ is its inverse.

The equations of motion, derived via the Newton-Euler or Lagrangian method, describe manipulator dynamics and form the basis for control, as follows [12]:

$$M(\mathbf{q})\ddot{\mathbf{q}} + \mathbf{c}(\mathbf{q},\dot{\mathbf{q}}) = \begin{bmatrix} \mathbf{0}_{3\times 1} \\ \boldsymbol{\tau}_m \end{bmatrix} \tag{4}$$

where $M(\mathbf{q}) \in \mathbb{R}^{6\times6}$ is the mass-inertia matrix, $\mathbf{c}(\mathbf{q}, \dot{\mathbf{q}}) \in \mathbb{R}^6$ is the vector of centrifugal and Coriolis terms, and $\boldsymbol{\tau}_m \in \mathbb{R}^3$ is the manipulator joint torques.

C. Orbital Mechanics

The primary objective of the manipulator motion is to impart a specific initial velocity to the Deputy at the release time, t_r, enabling it to intercept the desired relative orbit around the Client after a designated transfer duration, t_f. This maneuver is modeled using the Clohessy-Wiltshire (CW) equations [13], which describe the linearized relative dynamics between two bodies in a circular orbit.

To ensure the Deputy reaches a targeted relative position $\delta\mathbf{r}_d$ at the end of the transfer period, the required initial relative velocity immediately after release, $\Delta\mathbf{v}$, is calculated as:

$$\Delta\mathbf{v} = \Phi_{rv}(t_f)^{-1} \left[\delta\mathbf{r}_d - \Phi_{rr}(t_f)\delta\mathbf{r}_0\right] \tag{5}$$

where $\delta\mathbf{r}_0$ is the relative position of the Deputy at t_r. This impulse is provided entirely by the manipulator's motion, after which the Deputy follows a passive trajectory. Here, the state transition matrices Φ_{rr} and Φ_{rv} for the duration t_f are given by:

$$\Phi_{rr}(t_f) = \begin{bmatrix} 4-3c_n & 0 & 0 \\ 6(s_n - nt_f) & 1 & 0 \\ 0 & 0 & c_n \end{bmatrix} \tag{6}$$

$$\Phi_{rv}(t_f) = \begin{bmatrix} \frac{s_n}{n} & \frac{2(1-c_n)}{n} & 0 \\ \frac{2(c_n-1)}{n} & \frac{4s_n - 3nt_f}{n} & 0 \\ 0 & 0 & \frac{s_n}{n} \end{bmatrix} \tag{7}$$

where $s_n = \sin(nt_f)$ and $c_n = \cos(nt_f)$. The parameter $n = \sqrt{\mu/R^3}$ is the mean motion of the Client for a reference orbit radius R, where μ is the Earth's gravitational parameter.

Once the Deputy is released at t_r, its orientation is assumed to remain constant throughout the transfer. This approach focuses on the precision of the initial impulse delivered by the manipulator to achieve the transition into the desired relative orbit.

D. Control Law

A feedback Nonlinear Model Predictive Control (NMPC) algorithm is employed to achieve EE position and velocity tracking [14]. In [15], NMPC is shown to be effective for controlling space manipulators, which are highly nonlinear systems. Traditional approaches, such as proportional-integral-derivative control, often struggle to guarantee stable performance in the presence of dynamic coupling. NMPC effectively tracks trajectory changes while predicting future disturbances, a capability demonstrated for a planar robotic system in [16]. In this work, the controller generates joint torques to match the EE state to the required $\Delta\mathbf{v}$ at t_r.

To reach the desired state at release, the cost function is split into two components: Guidance and Release, where the subscripts g and r represent Guidance and Release, respectively. The controller targets a smooth guidance trajectory until the release time enters the prediction horizon, at which point it prioritizes the terminal release states. The cost function is defined as:

$$J_{\text{cost}} = \beta\mathbf{e}_r^T Q_r \mathbf{e}_r + \int_t^{t+t_h} \left[\dot{\mathbf{u}}^T R \dot{\mathbf{u}} + (1-\beta)\mathbf{e}_g^T Q \mathbf{e}_g\right] dt \tag{8}$$

where Q, $Q_r \in \mathbb{R}^{4\times4}$, and $R \in \mathbb{R}^{3\times3}$ are positive definite weighting matrices. The term t_h denotes the prediction horizon. The transition factor $\beta = \text{clip}[(t+t_h-t_r)/t_h, 0, 1]$ ensures a smooth shift between Guidance and Release modes without discontinuity.

The Release error $\mathbf{e}_r \in \mathbb{R}^4$ and Guidance error $\mathbf{e}_g \in \mathbb{R}^4$ are defined as:

$$\mathbf{e}_{r,g} = \begin{bmatrix} \mathbf{r}_{E_{r,g}/N} - \mathbf{r}_{E/N} \\ \mathbf{v}_{E_{r,g}/N} - \mathbf{v}_{E/N} \end{bmatrix} \tag{9}$$

where $\mathbf{r}_{E/N}$ and $\mathbf{v}_{E/N}$ represent the actual EE state. The desired terminal state at release, $\mathbf{r}_{E_d/N}$ and $\mathbf{v}_{E_d/N}$ ($\mathbf{v}_{E_d/N} = \Delta\mathbf{v}$), are determined by the orbital requirements in Eq. (5).

The guidance trajectory $\mathbf{r}_{E_g/N}$ is defined by a cubic polynomial:

$$\mathbf{r}_{E_g/N}(t) = \mathbf{r}_0 + \mathbf{v}_0 t + \alpha_2 t^2 + \alpha_3 t^3 \tag{10}$$

which leads to

$$\mathbf{v}_{E_g/N}(t) = \mathbf{v}_0 + 2\alpha_2 t + 3\alpha_3 t^2 \tag{11}$$

Here, $\mathbf{r}_0$ and $\mathbf{v}_0$ are the initial EE position and velocity, respectively. The coefficients are derived to satisfy the boundary conditions at t_r:

$$\alpha_2 = \frac{3(\mathbf{r}_{E_d/N} - \mathbf{r}_0) - (2\mathbf{v}_0 + \mathbf{v}_{E_d/N})t_r}{t_r^2} \tag{12}$$

$$\alpha_3 = \frac{2(\mathbf{r}_0 - \mathbf{r}_{E_d/N}) + (\mathbf{v}_0 + \mathbf{v}_{E_d/N})t_r}{t_r^3} \tag{13}$$

The controller predicts the system states over t_h and minimizes Eq. (8) to find the optimal control sequence $\mathbf{u}^* = [\mathbf{u}_0^*, \mathbf{u}_1^*, \ldots, \mathbf{u}_{t_h}^*]$. Following the receding horizon principle, only the first torque command is applied:

$$\boldsymbol{\tau}_m = \mathbf{u}_0^* \tag{14}$$

The optimization is repeated at each time step, using state feedback to reject disturbances arising from the base-manipulator dynamic coupling.

E. Simulation Model

To evaluate the dynamic interaction between the Chief, the manipulator, and the Deputy, a high-fidelity MATLAB simulation environment was developed. Because ground-based testing cannot fully replicate the microgravity conditions of space, the simulation serves as the primary platform for assessing system dynamics and validating the NMPC strategy. As shown in Fig. 3, the model is composed of the base satellite, a Kinova Gen3 7-DOF arm, a Robotiq 2f-140 rigid

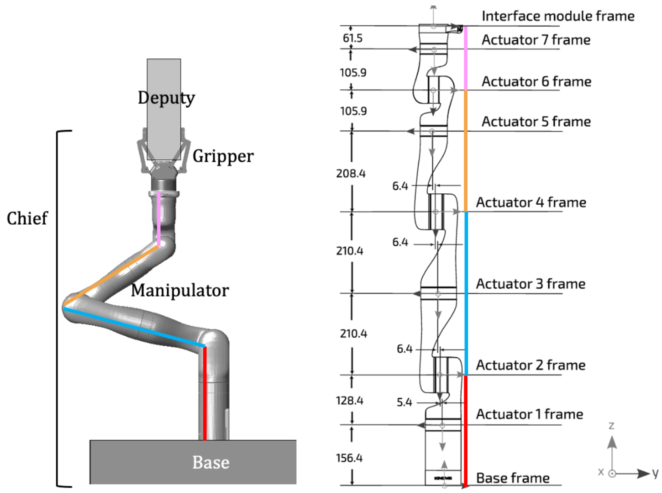

Fig. 3. Geometric simplification of Kinova Gen3: (left) 4-link planar model configuration and (right) original 7-DOF actuator frame dimensions.

two-finger gripper, and the Deputy satellite designated for deployment.

To maintain computational efficiency while capturing the essential non-holonomic coupling, the 7-DOF Kinova Gen3 is treated as a 4-link planar arm, using physical parameters and mass properties from [17].

IV. Simulation Study

Addressing a problem of this complexity requires comprehensive simulation and numerical analysis to identify feasible deployment solutions. In this study, a high-fidelity MATLAB simulation environment is utilized to analyze how the dynamic coupling between the manipulator and the free-floating base affects the Deputy's trajectory. The simulation parameters are closely modeled to match actual hardware systems. Additional information about initial conditions and simulation configuration is found in Table I. This approach enables characterization of realistic interactions between the manipulator and the Chief, providing insights into the precision of the NMPC-based "throwing" maneuver.

The primary scope of this work is to evaluate the feasibility of providing the required initial impulse to the Deputy solely through the manipulator's motion, eliminating the need for immediate onboard thruster burns. Consequently, the simulation focuses on the precision of the Deputy's state at the release time and propagates the resulting orbital trajectory over a designated transfer duration to assess intercept accuracy.

The deployment sequence consists of several key phases, as demonstrated in Fig. 4. Initially, the Chief rigidly grasps the Deputy, assuming no external disturbances. As the simulation progresses, the EE follows a cubic guidance trajectory toward the release point. Once the release time enters the NMPC prediction horizon, the controller shifts priority to minimizing the terminal release error. Upon reaching the target state, the gripper releases the Deputy, which then follows a passive orbital trajectory governed by CW dynamics.

TABLE I
Simulation Parameters

Parameter	Value	Unit
Base Mass	132	kg
Arm Mass	8.08	kg
Gripper Mass	1.025	kg
Deputy Mass	3	kg
Release Time	10	s
Transfer Duration	3	hr
Sampling Time	0.05	s
Prediction Horizon	1	s
Joint 2 Initial Angle	75	deg
Joint 3 Initial Angle	-130	deg
Joint 4 Initial Angle	55	deg
Desired Release Position (N Frame)	$[1.5\ 0.1]^T$	m
Desired Release Velocity (N Frame)	$[0.1248\ 0.0827]^T$	m/s
Client Location (N Frame)	$[1000\ 0]^T$	m

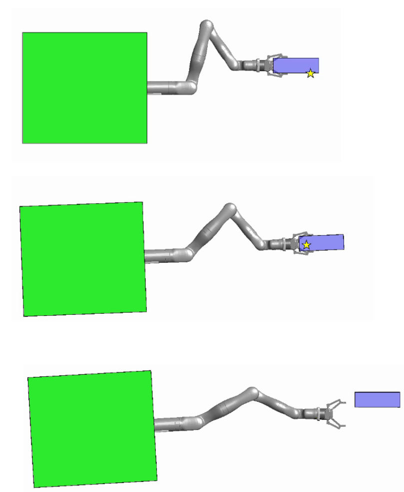

Fig. 4. Demonstration of throwing motion to release a Deputy.

TABLE II
Release Error of the NMPC

State Variable	Release Error	Terminal Error
Position	~ 0.011 cm , 0.07%	$<$30 cm
Velocity	~ 0.0002 cm/s , 0.02%	–
Orientation	~ 0.005 deg , 0.50%	–
Angular Velocity	~ 0.087 deg/s , 8.71%	–

The EE tracks the guidance trajectory towards the desired release state.The actual EE position and velocity closely match the guidance profiles, as seen in Fig. 5. The deviation observed at the end of the guidance phase corresponds to the transition toward prioritizing the release state over path-following.

The NMPC maintains sub-millimeter accuracy despite the dynamic coupling from the free-floating base, as summarized in Table II. By modeling the deputy's trajectory after the release from Fig. 5 for three hours, the Deputy reaches a point just 29 cm from the desired intercept point on the Desired Deputy Orbit (Fig. 6), which is well within the 10 m mission requirements. This demonstrates that the Release mode successfully prioritized the critical states to minimize drift during the orbital transfer window.

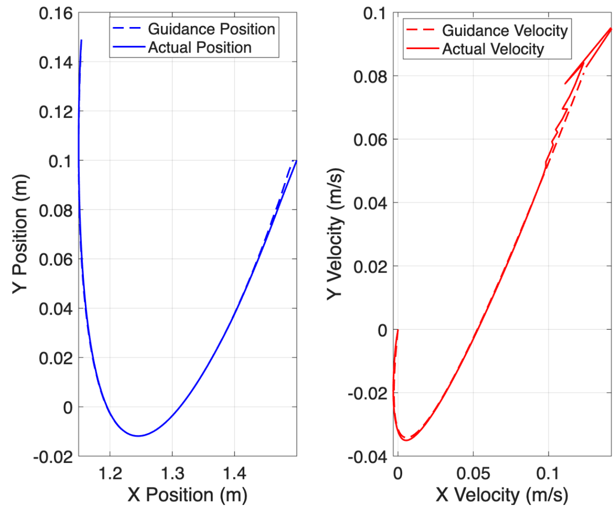

Fig. 5. Evolution of the EE position and velocity compared to the expected guidance trajectory phase.

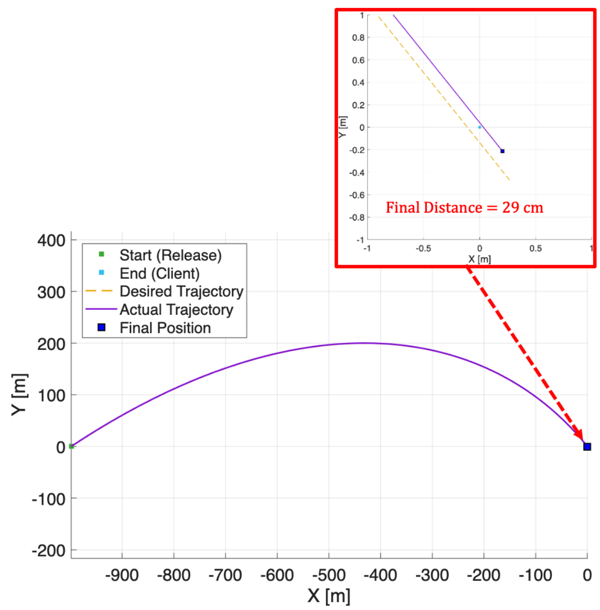

Fig. 6. Propagation of Deputy trajectory after release, considering a passive system.

To examine the robustness of the proposed algorithm, a Monte Carlo simulation was conducted using 100 randomized initial joint configurations. A simulation run is defined as successful if the final state is bounded within a 10 m radius from the Desired Deputy Orbit point relative to the Client (corresponding to $(0, 0)$ in the Hill frame). Based on this criterion, Fig. 7 illustrates that 99% of the test cases land within the 10 m boundary at the 3 hour mark. The single remaining trajectory is approximately 21 m away at this cut-off time. However, extending the propagation time by an additional 4 minutes brings this worst-case trajectory within the 10 m boundary, as shown in Fig. 8. The complete statistical summary of the Monte Carlo simulation is provided in Table III.

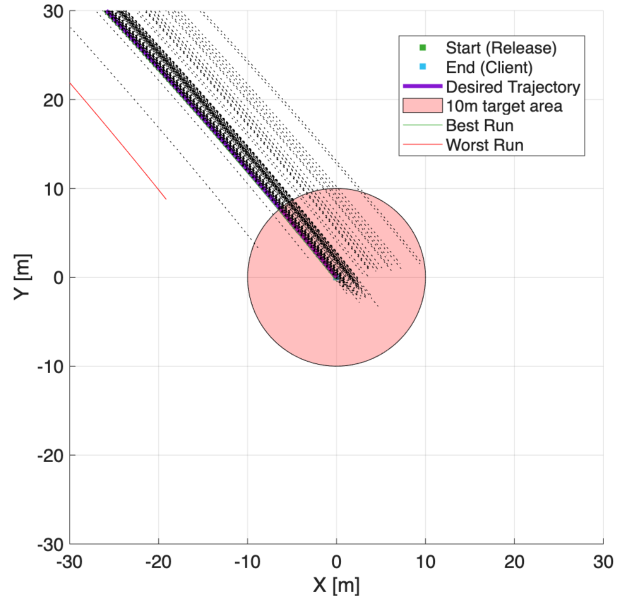

Fig. 7. Monte Carlo CW propagation of 100 Deputy trajectories following release from different initial joint configurations.

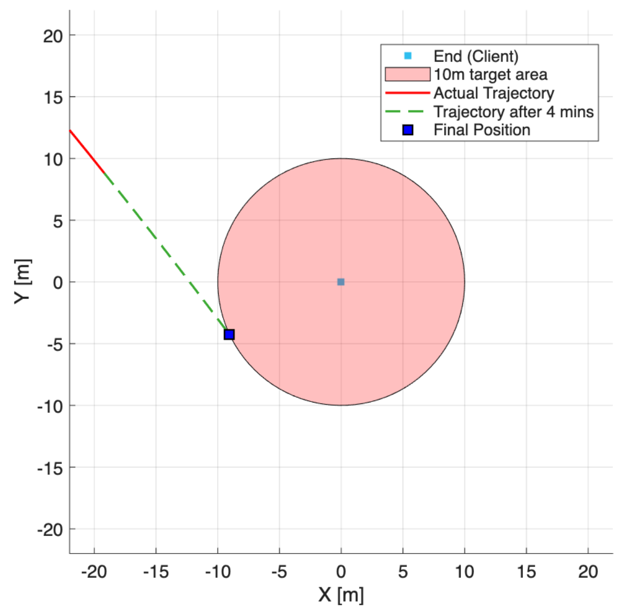

Fig. 8. The worst-case Monte Carlo trajectory propagated for an additional 4 minutes beyond the initial 3 hours.

TABLE III
MONTE CARLO STATISTICS

Statistic	Release Error		Terminal Error
	Position (cm) (X, Y)	Velocity (cm/s) (V_x, V_y)	Euclidean Norm (m)
Best	$(0.015, 0.002)$	$(0.001, 0.001)$	0.422
Worst	$(4.429, 2.583)$	$(0.152, 0.073)$	9.98*
Median	$(0.128, 0.111)$	$(0.014, 0.008)$	2.42
Average	$(0.259, 0.174)$	$(0.019, 0.014)$	3.12

*Based on an additional 4 minutes of passive flight.

V. Conclusion

This paper presents a new deployment approach that utilizes a "throwing" manipulation motion to impart a specific delta-v to a Deputy satellite, enabling it to reach a desired relative orbit without the immediate use of onboard thrusters. By utilizing a hybrid cost function to blend two objectives, the NMPC allows the Deputy to reach the desired orbit around the Client within 30 cm without additional onboard thrust. Future work will extend the planar control logic to three-dimensional motion and explore the implementation of an active free-flying Chief controller to assess the robustness of this approach across a wider range of mission scenarios.

Acknowledgment

The authors would like to thank Diego Quevedo for insightful discussions and contributions.

References

[1] D. J. Kessler, N. L. Johnson, J. Liou, and M. Matney, "The kessler syndrome: Implications to future space operations," Advances in the Astronautical Sciences, vol. 137, no. 8, pp. 47–61, 2010.

[2] R. Thirsk, A. Kuipers, C. Mukai, and D. Williams, "The space-flight environment: the international space station and beyond," Canadian Medical Association Journal, vol. 180, no. 12, pp. 1216–1220, 2009.

[3] I. G. E. Grossman and R. Verker, "Debris/micrometeoroid impacts and synergistic effects on spacecraft materials," Materials Research Society Bulletin, vol. 35, no. 1, pp. 41–47, 2010.

[4] Y. Lu, Q. Shao, H. Yue, and F. Yang, "A review of the space environment effects on spacecraft in different orbits," IEEE Access, vol. 7, pp. 93 473–93 488, 2019.

[5] D. Choi and D. Kim, "Minimal delta-v autonomous spacecraft inspection using genetic fuzzy-driven control," International Journal of Aeronautical and Space Sciences, vol. 27, pp. 2473–2487, 2026.

[6] A. N. Knight, T. R. Tetterton, A. J. Engl, P. M. Sinkovitz, B. J. Ward, and J. S. Kang, "Design and development of on-orbit servicing cubesat-class satellite," in Proceedings of the 34th Annual Small Satellite Conference, no. SSC20-WK-03. Virtual: Utah State University, August 2020.

[7] A. R. Tummala and A. Dutta, "An overview of cube-satellite propulsion technologies and trends," Aerospace, vol. 4, no. 4, p. 58, 2017.

[8] G. Hu, Y. Li, X. Li, G. Zhang, Z. Zhang, X. Wang, and W. Man, "Modular self-reconfigurable spacecraft: Development status, key technologies, and application prospect," Acta Astronautica, vol. 207, pp. 240–256, 2023.

[9] I. Hatty, "Viability of on-orbit servicing spacecraft to prolong the operational life of satellites," Journal of Space Safety Engineering, vol. 9, no. 2, pp. 263–268, 2022.

[10] D. Arney, J. Mulvaney, C. Williams, C. Stockdale, N. Gelin, and P. le Gouellec, "In-space servicing, assembly, and manufacturing (isam) state of play 2023," NASA, Technical Report, October 2023. [Online]. Available: https://www.nasa.gov/wp-content/uploads/2023/10/isam-state-of-play-2023.pdf

[11] S. Corpino and F. Stesina, "Inspection of the cis-lunar station using multi-purpose autonomous cubesats," Acta Astronautica, vol. 175, pp. 591–605, 2020.

[12] M. Wilde, S. Kwok Choon, A. Grompone, and M. Romano, "Equations of motion of free-floating spacecraft-manipulator systems: an engineer's tutorial," Frontiers in Robotics and AI, vol. 5, p. 41, 2018.

[13] H. Curtis, Orbital Mechanics for Engineering Students, 4th ed., ser. Elsevier Aerospace Engineering Series. Oxford, United Kingdom: Butterworth-Heinemann, 2020, pp. 365–376.

[14] D. Quevedo, S. Hudson, and D. Kim, "Modeling and control framework for autonomous space manipulator handover operations," in AAS/AIAA Astrodynamics Specialist Conference, Boston, MA, August 10–14 2025, available via arXiv:2508.18039 [cs.RO].

[15] Z. Guo, H. Ju, C. Lu, and K. Wang, "Dynamic modeling and improved nonlinear model predictive control of a free-floating dual-arm space robot," Applied Sciences, vol. 14, no. 8, p. 3333, 2024.

[16] T. Rybus, K. Seweryn, and J. Z. Sasiadek, Nonlinear Model Predictive Control (NMPC) for Free-Floating Space Manipulator. Cham, Switzerland: Springer International Publishing, 2018, pp. 17–29.

[17] Kinova® Gen3 Ultra lightweight robot User Guide. [Online]. Available: https://www.kinovarobotics.com/uploads/User-Guide-Gen3-R07.pdf